nature geoscience

SUPPLEMENTARY INFORMATION

DOI: 10.1038/NGEO724

*Site Information:*

Table S1:

| Sites | Modern Location | Modern SST (˚C) | PO4(μM)-0m | PO4(μM)-75m | |
|---|---|---|---|---|---|
| 130-806 | 0.5N, 159.5E | 29.2 | 0.24 | 0.34 | *(*6*) |
| 154-925 | 4.5N, 43.5W | 27.4 | 0.24 | 0.35 | *(*S35*) |
| 198-1208 | 36.5N, 158.5E | 18.2 | 0.24 | 0.50 | *(*S36*) |
| 167-1012 | 32.5N, 118.5W | 16.2 | 0.41 | 0.97 | *(*5*) |
| 162-982 | 57.5N, 16W | 11.6 | 0.37 | 0.61 | *(*S35*) |
| 145-882 | 50.3N, 167.5E | 6.2 | 1.26 | 1.92 | *(*S37*) |

*References *5, 6*, and *S35-37* provide age models for each site

---

*Calculation of alkenone-based [$CO_{2aq}$]*

Alkenone-$CO_2$ estimates are based on the expression:

$$\varepsilon_{p37:2} = \varepsilon_f - b/[CO_{2aq}] \quad (1)$$

where the term "*b*" represents the sum of physiological factors, including growth rate and cell geometry, that affect total carbon isotope discrimination. $\varepsilon_f$ represents the carbon isotope fractionation due to all carbon-fixing reactions. $\varepsilon_{p37:2}$ is the carbon isotopic differences between $CO_{2aq}$ and the algal cell equivalent to:

$$\varepsilon_{p37:2} = [(\delta_{CO2aq} + 1000)/(\delta_{org} + 1000)-1]10^3 \quad (2)$$

where $\delta_{org}$ is the carbon isotopic composition of the algal cell estimated from the stable isotopic compositions of alkenones ($\delta_{37:2}$) :

$$\delta_{org} = [( \delta_{37:2} +1000)*((4.2/1000)+1)]-1000 \quad (3)$$

$\delta_{CO2aq}$ represents the $\delta^{13}C$ of ambient $CO_{2aq}$, approximated from the $\delta^{13}C$ of shallow-dwelling foraminifera assuming isotopic and chemical equilibria among all the aqueous inorganic carbon species, atmospheric $CO_2$, and foraminiferal calcite. Values of '*b*' in Equation 1 are correlated to surface-water [$PO_4^{3-}$] in surface waters of the modern ocean and yield the relationship:

$$[CO_{2aq}] = (116.96[PO_4^{3-}]+81.41)/(25-\varepsilon_{p37:2}) \quad (4)$$

[$CO_{2aq}$] is converted to atmospheric $CO_2$ concentration by applying Henry's Law *(S31)* assuming a salinity of 35, and using mixed-layer $U^{K'}_{37}$-based temperatures. Analytical treatment of error propagation suggests a ~20% uncertainty for reconstructed [$CO_{2aq}$] during this time interval *(S32)*.

The '*b*' versus [$PO_4^{3-}$] relationship is a geometric mean regression of all available data from particulate organic matter using $\varepsilon_f$ = 25‰ *(23,S33)* (*Fig. S1*). Regional expressions for the physiology-dependent term '*b*' can be constructed that deviate from the global regression. As such, regional effects

DOI: 10.1038/NGEO724

can contribute to differences in $CO_2$ estimates from site to site. In an attempt to explain data that strongly deviate from the global '*b*' versus [$PO_4^{3-}$] regression, Eek *et al. (S34)* argued that the $\varepsilon_p$ versus [$PO_4^{3-}$] relationship is robust when $NO_3$+$NO_2$ ([N]) is greater than zero, but fails when [N] = 0. While data from some low [N] environments (i.e., Hawaiian Ocean Time Series, Bermuda Atlantic Time Series) lend support to this supposition, low [N] data from the equatorial Indian Ocean and the Arabian Sea do not. To date, the totality of factors responsible for the scatter remains unknown.

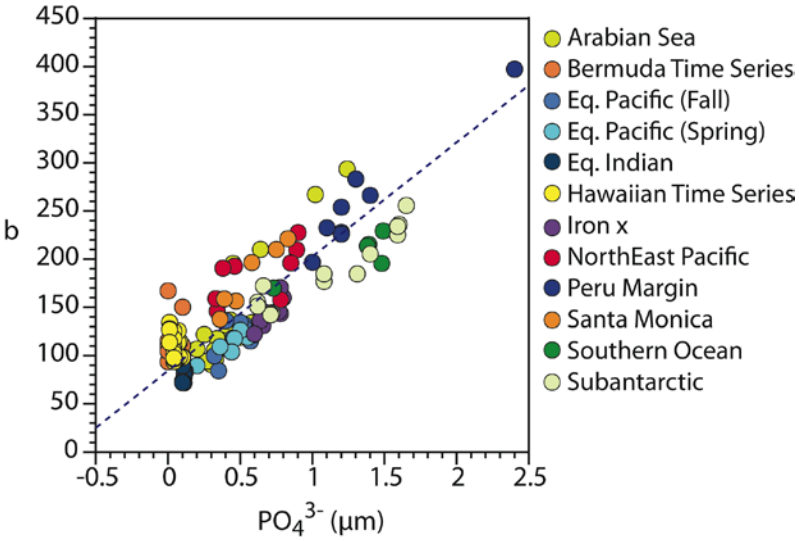


Figure S1. Compilation of '*b*' versus soluble phosphate for natural haptophyte populations (see *23*, *S33* for references). Solid line represents the geometric mean regression.

*Temperature and $\varepsilon_{p37:2}$ trends at each site*

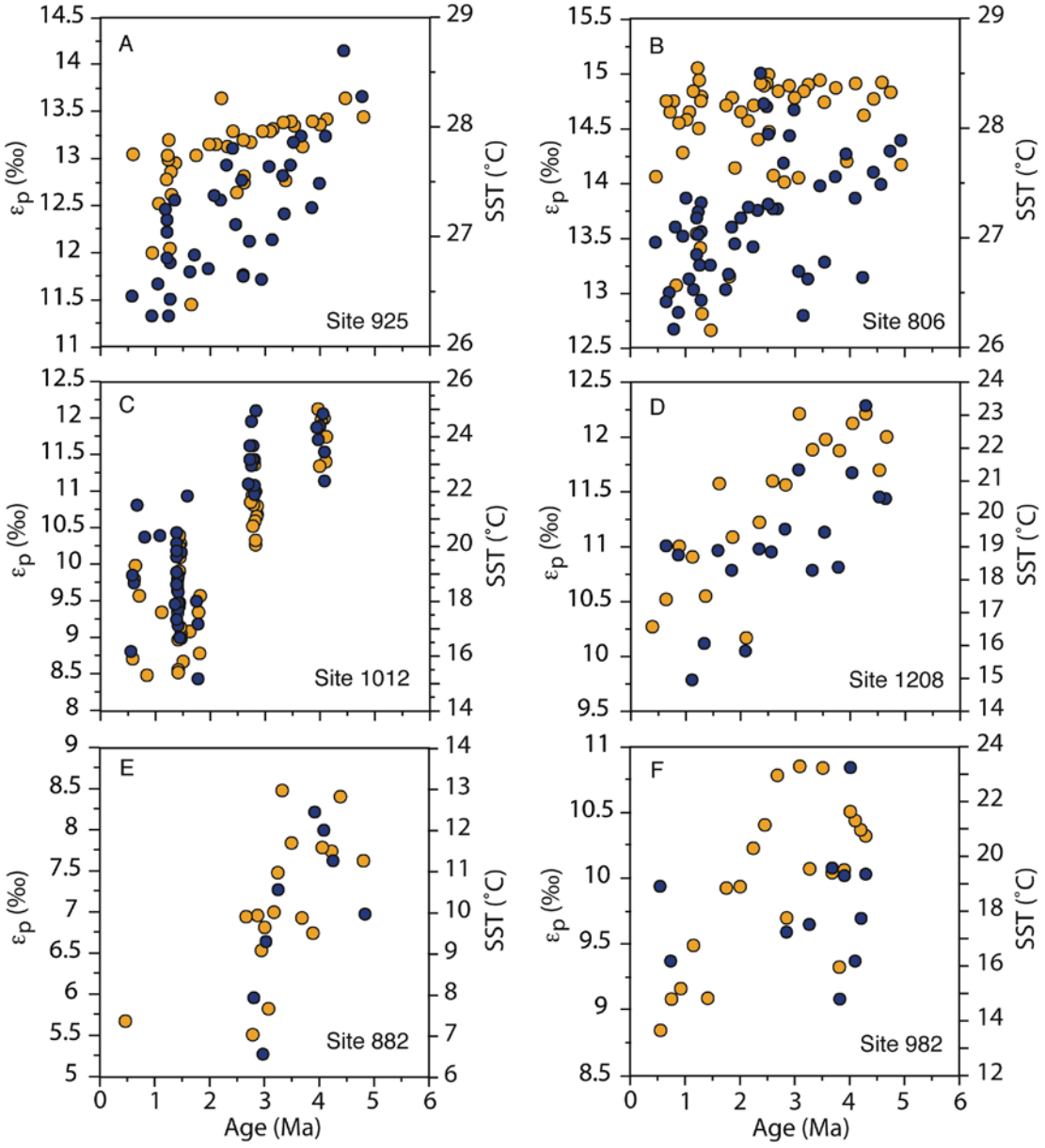


Figure S2. $\varepsilon_{p37:2}$ values and sea-surface temperatures. Alkenone SST temperatures (orange circles) are associated with an uncertainty of at least ±1.1˚C based on the global $U^{K'}_{37}$-SST calibration. Analytical uncertainty of $\varepsilon_{p37:2}$ values (blue circles) is ±0.4‰ or better based on the standard error of $\delta^{13}C_{37:2}$ measurements. Note that scales differ between panels.

*Comparison between previously published alkenone-based $CO_2$ records*

Previously published alkenone-based $CO_2$ estimates *(28)* indicate that $CO_2$ increased from ~200 to ~300 ppm from 15 to 5 million years ago (Fig. S2*)*. Rising $CO_2$ levels for several million years prior to

DOI: 10.1038/NGEO724

the early Pliocene is consistent with evidence for peak warming during this time. However, $CO_2$ estimates for the Pliocene are higher than those published in *Pagani et al. (27)*. Differences between these $CO_2$ records have several probable causes including differences in air-sea equilibrium between sites, depth of production and irradiance, regional expressions of the '*b*' versus [$PO_4^{3-}$] calibration, and temperature reconstructions. In addition, temperature estimates in *Pagani et al. (27)* were reconstructed from planktonic foraminiferal $\delta^{18}O$ values coeval with alkenone $\delta^{13}C$ measurements. These $\delta^{18}O$ temperature estimates are impacted by estimates of ice-volume, depth of calcification, and the degree of carbonate diagenesis. In contrast, for this study we apply alkenone-based temperatures, which increase the fidelity of our temperature estimates, as well as an updated '*b*' versus [$PO_4^{3-}$] calibration (*S33*; Eq. 4). Site 806 alkenone-based temperatures are ~6˚C warmer during the earliest Pliocene (this study) compared to $\delta^{18}O$-based temperature estimates used to calculate late Miocene $CO_2$ levels at Site 588 (*S33*). Indeed, new $Tex_{86}$ temperature estimates for Site 588 during the early Pliocene (*Pagani, unpublished*) suggest that Site 588 SSTs were as much as 8˚C warmer than temperatures inferred from planktonic $\delta^{18}O$ records. If higher temperature estimates are applied at Site 588, much of the $CO_2$ offset between our current and previously published $CO_2$ records can be accounted for (Fig. S2).

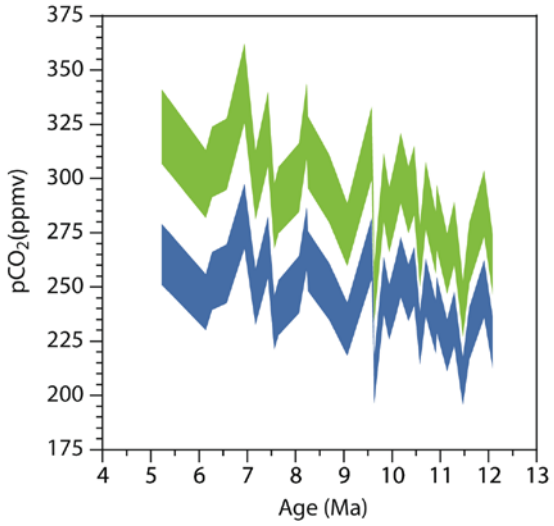


Figure S3. Alkenone-based $CO_2$ estimates from Site 588. This figure demonstrates the effect of different temperature estimates on the calculated value of $CO_2$. 'Blue' values are estimated using $\varepsilon_{p37:2}$ values and foraminifera-based temperature estimates published in (*27*), but using an updated '*b*' versus [$PO_4^{3-}$] calibration (Eq. 4). 'Green" $CO_2$ values assume SSTs are warmer than those predicted from shallow-dwelling foraminifera. Temperature offsets are assumed to linearly increase from 12 to 5 Ma, with early Pliocene SSTs 8˚C warmer than $\delta^{18}O$-based temperatures and only 6˚C warmer (previously assumed in reference *S33*) at 12 Ma.

*Calculation of $CO_{2slope}$ and Pliocene $CO_2$*

Atmospheric carbon dioxide concentrations for the middle to early Pliocene were estimated by calculating maximum and minimum ranges of $CO_2$ using reconstructed $\varepsilon_{p37:2}$ values (Eq. 4), a range of $[PO_4^{3-}]$ values for each sites (Table S1), and $U^{K'}_{37}$ sea-surface temperatures (Fig. S2). Each site is influenced by different oceanographic properties that result in differences in the concentration of $CO_2$. However, long-term changes in atmospheric $CO_2$ would impart a similar temporal $CO_2$ change at each site. Long-term change in $CO_2$ is assessed by calculating individual linear regressions through maximum and minimum estimates of $CO_2$ ($CO_{2slope}$). We take these linear regressions as reflecting both the long-term change in atmospheric carbon dioxide and regional oceanographic/biological effects that alter the expression of global $CO_2$ change at each site. We then refine $CO_2$ estimates by considering probable site-specific changes in oceanographic conditions through time that impact $CO_{2slope}$. For high-latitude Site 982 we assume upper-water column stratification change, due to a change in temperature, which would have allowed for higher rates of nutrient supply and higher productivity at this site (*Kira Lawrence, pers. comm.*) in the early Pliocene compared to modern conditions, we assume the $CO_{2slope}$ increased from the lower regression (low $[PO_4^{3-}]$) at 0 Ma to the upper regression (high $[PO_4^{3-}]$) at 4.5 Ma. Similarly, we assume $CO_{2slope}$ from tropical Sites 806 and 925, and subtropical Site 1208 increases due to enhanced vertical mixing during the warm early Pliocene. The magnitude of $CO_{2slope}$ change at Site 1208 is assumed less extreme given its distance from the tropical warm pool. Accordingly, $CO_{2slope}$ at this site is modeled by using the maximum $CO_2$ concentration at 4.5 Ma calculated using the average of the maximum and minimum $[PO_4^{3-}]$ values and the minimum $CO_2$ value at 0 Ma. Finally, seasonal upwelling at Site 1012 during the earliest Pliocene was reduced *(17,25*) and then increased toward the Present. We model a reduction in $CO_{2slope}$ at Site 1012 by assuming nutrient concentrations at 4.5 Ma are represented by the average between the maximum and minimum $[PO_4^{3-}]$ values and the highest $[PO_4^{3-}]$ at 0 Ma.

*Alternative nutrient and $CO_{2slope}$ scenario for Site 1012*

Atmospheric carbon dioxide concentrations at Site 1012 were calculated using a modern range of $[PO_4^{3-}]$ (Fig. 2C). Today, Site 1012 is characterized by seasonal upwelling. However, during the early Pliocene, seasonal upwelling was probably reduced *(17,25)* and then increased toward the Present. For the $CO_2$ trend implied by the arrow in Figure 2c, we assume that early Pliocene haptophyte production occurred at a depth between 0 and 75 m and apply the concentration of $PO_4^{3-}$ that is the average between maximum and minimum values (Table S1). This assumption leads to early Pliocene $CO_2$ estimates that are higher than if production is assumed to have occurred at the sea-surface (for example, compare "lines" 3 and 1 in Fig. S4). However, if haptophyte production always occurred close to the surface and the rate of seasonal upwelling (and the concentration of surface-water $PO_4^{3-}$) was lower during the early Pliocene,

DOI: 10.1038/NGEO724

then the magnitude of early Pliocene $CO_2$ would be lower than that calculated in Figure 2c. In order to assess the effect of even lower nutrient concentrations (and an assumption of lower haptophyte growth rates) during the early Pliocene, we re-evaluate $CO_2$ estimates at Site 1012 by assuming early Pliocene [$PO_4^{3-}$] was only 0.25 µM at 4.5 Ma and increased to 0.41µM by 0 Ma (Fig. S4). This treatment results in a slightly lower $CO_{2slope}$ and a maximum $CO_2$ change of 92 ppm since preindustrial times (black arrow in Fig. S4) compared with 128 ppm (grey arrow in Figure S4.). This alternative scenario also reduces the overall possible range of early Pliocene $CO_2$ (dashed green line in Fig. 3).

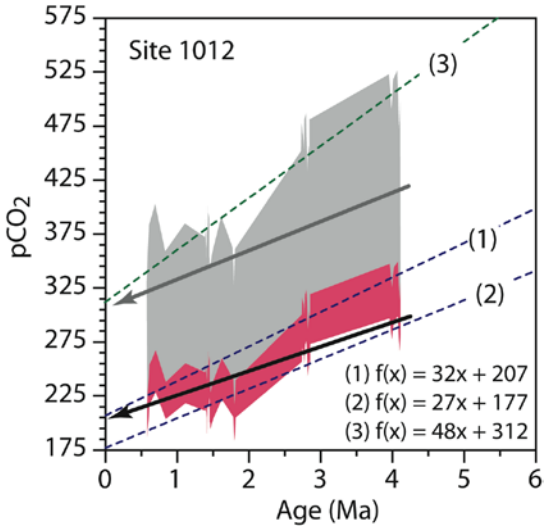


Figure S4. Alternative $CO_2$ calculations for Site 1012. Data shaded grey and grey arrow represents estimates of $CO_2$ and $CO_{2slope}$. $CO_2$ estimates in red represent an alternative scenario that assumes constant surface-water haptophyte production and lower-than-modern [$PO_4^{3-}$] during the early Pliocene ([$PO_4^{3-}$] = 0.25µM). This new scenario for site 1012 yields a lower $CO_{2slope}$ (black arrow) and predicts a slightly smaller change in $CO_2$ since 4.5 million years ago.

References

S31. Weiss, R. F. Caron dioxide in water and seawater: the solubility of a non-ideal gas. *Mar. Chem.* **2**, 203-215 (1974).

S32. Freeman, K.H., Pagani, M., Alkenone-based estimates of past $CO_2$ levels: a consideration of their utility based on an analysis of uncertainties. In *A History of Atmospheric $CO_2$ and its Effects on Plants, Animals, and Ecosystems,* J. R. Ehleringer, T. E. Cerling, and M. D. Dearing, Eds. (Springer, New York, 2005), pp. 35-61.

S33. Pagani, M., Zachos, J. C., Freeman, K. H., Tipple, B., Bohaty, S. Marked decline in atmospheric carbon dioxide concentrations during the Paleogene. *Science* **309**, 600-603 (2005).

S34. Eek, M.E., Whiticar, M.J., Bishops, J.K.B., Wong, C.S. Influence of nutrients on carbon isotope fractionation by natural populations of Prymnesiophyte algae in NE Pacific. *Deep-Sea Research II*, **46**, 2863-2876 (1999).

S35. Lisiecki, L.E. & Raymo, M.E. A Pliocene-Pleistocene stack of 57 globally distributed benthic $\delta^{18}O$ records. *Paleoceanography* **20**, PA1003 (2005).

S36. Shipboard Scientific Party, Proc. *Proc. ODP, Init. Rep.* **198**, Chapter 4 (2002).

S37. Tiedemann, R. & Haug, G. H. Astronomical calibration of cycle stratigraphy for Site 882 in the northwest Pacific. In Rea, D.K., Basov, I.A., Scholl, D.W., and Allen, J.F. (Eds.), *Proceedings Ocean Drilling Program Scientific Results*, 145, 283-292 (1995).